



Study on the Effect of Particle Shape on the Soil-Rough Interface Shearing Using 3D DEM

Xue-Ying Jing and Wan-Huan Zhou^(✉)

University of Macau, Macau, China
hannahzhou@umac.mo

Abstract. The soil-structure interface (SSI) is involved in many aspects of geotechnical engineering, with a range of efforts having been made to investigate the factors influencing its mechanical behavior. Its shear resistance and volumetric change are mainly governed by the soil properties. The particle shape emerges as an essential soil property affects various mechanical behaviors of the bulk soil, in terms of its compactness, the rotation of the particles, its shearing resistance, and so on. The particle shape effect must be properly considered as it pertains to the SSI issue. In this study, the interface shear tests are modeled using the three-dimensional (3D) discrete element method (DEM). Three types of clustered elements are used to represent the irregular particles, with the same relative density of the specimen being controlled before shearing. The effects of particle shape on the shear stress and volumetric deformation were analyzed, the specimen consisting of irregular elements showing a higher shearing resistance and larger dilation than the one consisting of spherical balls. The localization of shearing deformation was also investigated, with the finding that the thickness of the localized band is approximately four times that of the medium particle diameter.

Keywords: Soil-structural interface · Particle shape · Relative density
Interface shear test

1 Introduction

The soil-structure interface (SSI) exists in many aspects of geotechnical engineering. Conventional studies to characterize the mechanical behavior of SSI mainly rely on laboratory and in-site experiments. Efforts have been made to investigate the factors influencing the mechanical behavior of SSI. It has been proven that the properties of the bulk soil [1, 2] play an important role in the shearing resistance of the soil subjected to an interface shearing, as well as the properties of structural interface, including the friction coefficient, geometry, roughness, and stiffness of the interface material [3–6].

A variety of investigations have revealed that the particle shape affects various mechanical behaviors of the bulk soil. The correlation between the extreme porosity of the soil and shape parameter has been explored [7, 8]. In addition, the rotation of particles of irregular shape is restricted and accordingly increases the interlocking inside the soil, which induces a higher shear strength and larger dilation [9]. In this

context, the particle shape emerges as an essential soil property that needs to be properly considered in the SSI issue.

Over the decades, the discrete element method (DEM) has been widely deployed in the geotechnical field. Both two-dimensional (2D) and three-dimensional (3D) DEM simulations have been successfully applied to the SSI issue [6, 10–12]. A benefit of this approach is that the microscopic physics of the particles can be obtained for analysis. The particle used in early DEM models was a disc in 2D and a spherical ball in 3D. Such an idealized granular system cannot properly reflect the real motions of the soil material, which is of irregular shape in nature. Thus, non-spherical elements have also been used in DEM simulations, such as clustered elements, polygons, and ellipsoids [13–17]. Jensen [12] employed clustered elements in a 2D SSI simulation. However, the way in which the particle shape affects the shear resistance of SSI and the evolution of microscopic quantities is yet to be fully studied.

In this study, an interface shearing test is modeled using 3D DEM. Three types of clustered elements are used to represent the irregular soil particles. This study was aimed at focusing on three aspects: (1) the extreme porosity of the specimens consisting of various elements, (2) the effect of particle shape on the macroscopic behaviors of SSI in the aspects of shear stress and volumetric change, and (3) the effect of particle shape on the localization of shearing deformation inside the specimen.

2 Numerical Model of PFC 3D

2.1 Interface Shear Test

PFC 3D 5.0 software (Itasca), based on the discrete element method [18], was employed in this study. The numerical model of the interface shear test is illustrated in Fig. 1. A regular saw-tooth wall was used to represent the rough interface. The normalized roughness R_n equals h/d_{50} in reference to the definition proposed by Uesugi and Kishida [19], in which d_{50} is the mean particle size. The specimen of a given porosity was generated inside the shear box. The bottom wall started to move in x -direction at a constant speed to induce an interface shearing. During the shearing process, the top wall was controlled by a servo system to maintain a constant normal stress σ_n . The shear stress τ is the shear force measured on the interface wall divided by

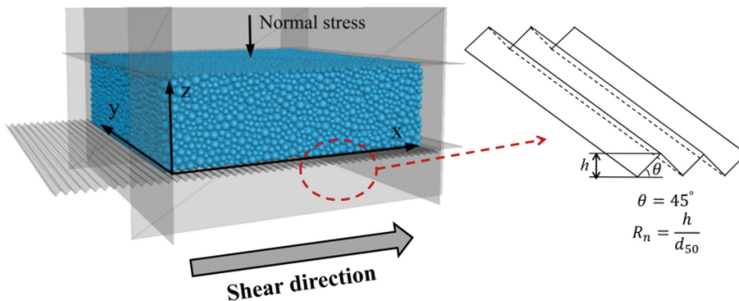


Fig. 1. The numerical model in the PFC 3D and the definition of normalized roughness R_n

the area of horizontal section of the shear box. The vertical displacement d_v of the top wall was recorded to reflect the volumetric change of the specimen.

2.2 Input Parameters and Local Contact Model

The non-linear Hertz-Mindlin contact law was used in this study. The input parameters, listed in Table 1, refer to the 3D simulation performed by Lin and Ng [13] using arrays of ellipsoids. A damping coefficient with a value of 0.7 was applied and a quasi-static analysis was guaranteed. It should be noted that to verify the validity of the model is significant for the DEM modeling. However, in this study, three different types of clustered particles have been used. The calibration for one type of clustered particles cannot represent the other two. Thus, we used the parameters which have been proven reasonable by the previous researchers.

Table 1. The input parameters of the numerical model

Input parameter	Value	Input parameter	Value
Dimension of shear box (mm ³)	100 × 100 × 30	Shear modulus G (GPa)	28.957
Normal stress σ_n (MPa)	50	Poisson's ratio ν	0.15
R_n of interface	0.5	Particle-particle friction coefficient μ_p	0.5
Shearing rate (mm/s)	0.015	Particle-interface friction coefficient μ_{pw}	0.2
Mean particle size d_{50} (mm)	2.7	Damping coefficient	0.7

2.3 Geometry of the Clustered Element

A clustered element, known as a clump, can be formed by adding certain particles together using overlapping. Three types of elements, spherical ball, elongated clump, and pyramid clump, were used in the model (Fig. 2). An equivalent diameter d_{eq} was denoted for the clumps with non-spherical shape, which were defined as the diameter of a spherical ball with the same volume of the clump. Three specimens, consisting of different elements, were prepared respectively. All specimens followed a linear grain size distribution in the range of 1.8–3.6 mm, as shown in Fig. 3.

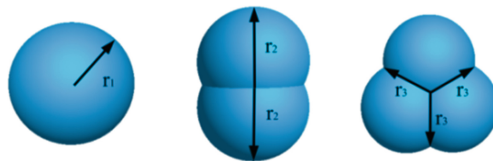


Fig. 2. Three types of elements (spherical ball, elongated clump, pyramid clump) used in the numerical model in the PFC 3D

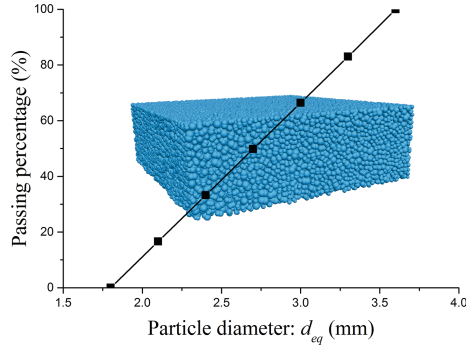


Fig. 3. The grain size distribution of the specimen

3 Macroscopic Responses

3.1 Extreme Porosity of the Specimen

The preparation of the specimen in this study followed the procedure proposed by Muir and Kenichi [20] to obtain the densest and loosest specimens consisting of various elements. The maximum porosity n_{max} and minimum porosity n_{min} of the specimens consisting of spherical balls, elongated clumps, and pyramid clumps respectively are listed in Table 2. It can be observed that the specimens consisting of non-spherical elements, especially the pyramid clump, tended to form a denser configuration. This result is consistent with the existing laboratory experiment [9]. The relative density D_r of the granular material was defined by Eq. 1. Three ISTs were modeled with the same initial relative density ($D_r = 90\%$) and the corresponding initial porosities n_0 are listed in Table 2.

$$D_r = \frac{(n_{max} - n)(1 - n_{min})}{(n_{max} - n_{min})(1 - n)} \quad (1)$$

Table 2. The extreme and initial porosities of the numerical tests

Test	Element	Maximum porosity: n_{max}	Minimum porosity: n_{min}	Relative density: D_r	Initial porosity: n_0
IST-S	Spherical ball	0.392	0.349	90%	0.353
IST-E	Elongated clump	0.356	0.291	90%	0.298
IST-P	Pyramid clump	0.361	0.279	90%	0.289

3.2 Evolutions of Shear Stress and Vertical Displacement

The macroscopic behaviors of the simulation are illustrated in Fig. 4. The evolutions of shear stress τ for the three ISTs showed a similar tendency: the stress-softening occurred after the peak shear stress τ_p was reached. The specimen consisting of non-spherical elements (elongated clump and pyramid clump) showed a higher peak shear stress τ_p than the one consisting of spherical balls. The difference in shearing resistance may correspond to interlocking between the particles, in which the rotations of the irregular clumps were restricted compared to those of the spherical balls. Thus, the interlocking was enhanced between inter-particles and between the particles and the rough interface. The critical shear stress of the IST-P was close to the one of IST-E, which was also higher than the one composed of spherical balls (IST-S). The evolution of vertical displacement of the top wall d_v reflected the volumetric changes of specimens. All specimens contracted at the commencement of shearing before gradually dilating. The growing rate of dilation slowed down at the shear displacement $d_s = 4$ mm, where the shear stress softening occurred. A stronger dilatancy was observed in the specimen with spherical balls. The results prove that both the shear resistance and volumetric change of the specimen are affected by the particle shape.

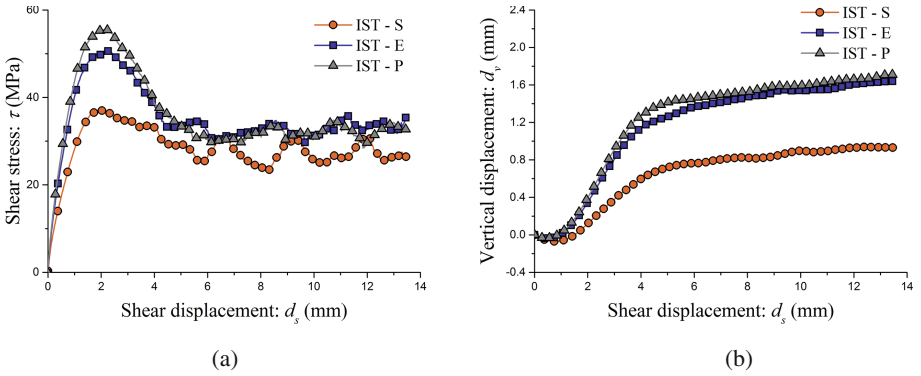


Fig. 4. Macroscopic responses of the ISTs ($D_r = 90\%$, $R_n = 0.5$): (a) shear stress τ versus shear displacement d_s and (b) vertical displacement d_v versus shear displacement d_s

4 Localization of the Shear Deformation

The benefit of the DEM simulation is that the movement of each particle can be traced and recorded. Certain measuring windows ($100 \text{ mm} \times 100 \text{ mm} \times 5 \text{ mm}$) are placed at different heights Z of the specimen to attain the average displacement of particles in the x -direction, which is denoted by d_x . The curve of the average shearing displacement d_x of particles, as a function of height Z , can be obtained at pre-peak shear stress, peak shear stress, post-peak shear stress, and steady shear stress (Fig. 5). At the beginning of shearing ($d_s = 1$ mm), the $d_x(Z)$ curves are approximately linear. At higher positions of the specimen, the spherical balls show a smaller value of d_x than the irregular particles. With the increasing of shear stress, the linear $d_x(Z)$ curves tend to become

non-linear. A narrow band is gradually localized on the bottom of the specimen, named the localized band. The inflection point can be found by analyzing the curvature κ of the curve, while the spherical particles at the higher position show negative displacement d_x at the steady stress state.

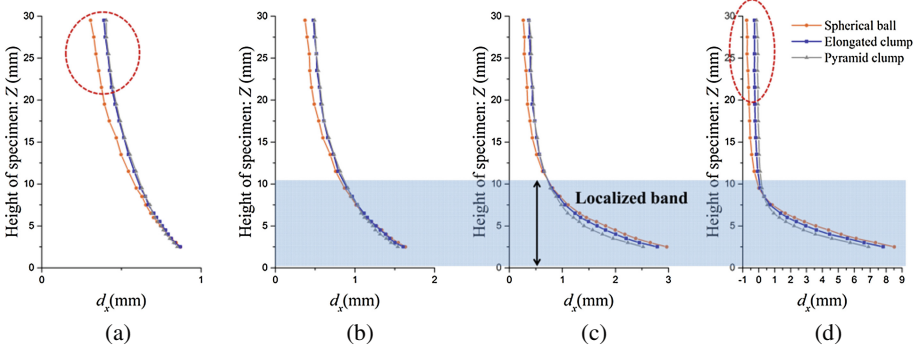


Fig. 5. The $d_x(Z)$ curves for the test IST-S, IST-E and IST-P at different stress state: (a) pre-peak shear stress ($d_s = 1$ mm), (2) peak shear stress ($d_s = 2$ mm), (3) post-peak shear stress ($d_s = 4$ mm), and (4) steady shear stress ($d_s = 13.5$ mm)

The inflection point of the curve of $d_x(Z)$ at the steady stress state (when $d_s = 13.5$ mm) is used to define the thickness of the localized band. Spline interpolation is applied to obtain a smooth d_x - Z curve $f(Z)$. The first derivative $f'(Z)$ and second derivative $f''(Z)$ are calculated using the finite difference method. The curvature κ of $f(Z)$ is calculated using Eq. 2:

$$\kappa = \frac{|f''(Z)|}{(1 + f'(Z)^2)^{3/2}} \tag{2}$$

The inflection point of the κ is considered a sign of the top boundary of the localized band. The authors suggest that the point where the κ equals 0.02 is the inflection point. The thickness of the localized band of the three ISTs is 10.5 mm (approximately four times that of the mean particle equivalent diameter at 2.7 mm).

5 Conclusions

The effect of particle shape on the shear behavior of the SSI was studied from macroscopic and microscopic mechanical viewpoints using 3D DEM simulations of ISTs consisting of spherical balls, elongated clumps, and pyramid clumps respectively. The following conclusions were drawn: (1) the specimens consisting of irregular clumps tend to form a denser configuration from an analysis of the extreme porosities of specimens; (2) the shear stress and volumetric change were affected by the particle shape. The IST consisting of irregular (pyramid and elongated) clumps shows a higher

shear resistance and larger dilation than the one consisting of spherical balls; and (3) the shear deformation is localized in a narrow band adjacent to the interface with the increasing of shear stress. The thicknesses of the localized bands for the three ISTs are approximately four times that of the mean particle equivalent diameter.

Acknowledgement. The authors wish to thank the financial support from the Macau Science and Technology Development Fund (FDCT) (125/2014/A3), the University of Macau Research Fund (MYRG2017-00198-FST, MYRG2015-00112-FST).

References

1. Zhu, H., Zhou, W.H., Yin, Z.Y.: Deformation mechanism of strain localization in 2D numerical interface tests. *Acta Geotechnica* (2017, In press)
2. Zhou, W.H., Yin, J.H., Hong, C.Y.: Finite element modelling of pullout testing on a soil nail in a pullout box under different overburden and grouting pressures. *Can. Geotech. J.* **48**(4), 557–567 (2011)
3. Uesugi, M., Kishida, H.: Influential factors of friction between steel and dry sands. *Soils Found.* **26**(2), 33–46 (1986)
4. Paikowsky, S.G., Player, C.M., Connors, P.J.: A dual interface apparatus for testing unrestricted friction of soil along solid surfaces. *ASTM Geotech. Test. J.* **18**(2), 168–193 (1995)
5. Jing, X.Y., Zhou, W.H., Zhu, H.X., Yin, Z.Y., Li, Y.M.: Analysis of soil-structural interface behavior using three-dimensional DEM simulations. *Int. J. Numer. Anal. Method. Geomech.* (2017, Accepted)
6. Frost, J.D., Dejong, J.T., Recalde, M.: Shear failure behavior of granular-continuum interfaces. *Eng. Fract. Mech.* **69**(17), 2029–2048 (2002)
7. Miura, K., Maeda, K., Furukawa, M., Toki, S.: Mechanical characteristics of sands with different primary properties. *Soils Found.* **38**(4), 159–172 (1998)
8. Nakata, Y., Kato, Y., Hyodo, M., Hyde, A.F., Murata, H.: One-dimensional compression behaviour of uniformly graded sand related to single particle crushing strength. *Soils Found.* **41**(2), 39–51 (2001)
9. Santamarina, J.C., Cho, G.C.: Soil behaviour: the role of particle shape. In: *Advances in Geotechnical Engineering*, vol. 1, pp. 604–617. Thomas Telford, London (2004)
10. Wang, J.F., Jiang, M.J.: Unified soil behavior of interface shear test and direct shear test under the influence of lower moving boundaries. *Granular Matter* **13**(5), 631–641 (2011)
11. Jing, X.Y., Zhou, W.H., Li, Y.M.: Interface direct shearing behavior between soil and saw-tooth surfaces by DEM simulation. *Procedia Eng.* **175**, 36–42 (2017)
12. Jensen, R.P., Bosscher, P.J., Plesha, M.E., Edil, T.B.: DEM simulation of granular media - structure interface: effects of surface roughness and particle shape. *Int. J. Numer. Anal. Meth. Geomech.* **23**(6), 531–547 (1999)
13. Lin, X., Ng, T.T.: A three-dimensional discrete element model using arrays of ellipsoids. *Géotechnique* **47**(2), 319–329 (1997)
14. Ni, Q., Powrie, W., Zhang, X., Harkness, R.: Effect of particle properties on soil behavior: 3-D numerical modeling of shearbox tests. In: *Numerical Methods in Geotechnical Engineering*, pp. 58–70 (2000)
15. Lu, M., McDowell, G.R.: The importance of modelling ballast particle shape in the discrete element method. *Granular Matter* **9**(1–2), 69–80 (2007)

16. Salot, C., Gotteland, P., Villard, P.: Influence of relative density on granular materials behavior: DEM simulations of triaxial tests. *Granular Matter* **11**(4), 221–236 (2009)
17. Bono, J.P., McDowell, G.R.: An insight into the yielding and normal compression of sand with irregularly-shaped particles using DEM. *Powder Technol.* **271**, 270–277 (2015)
18. Cundall, P.A., Strack, O.D.L.: A discrete numerical model for granular assemblies. *Géotechnique* **29**(1), 47–65 (1979)
19. Uesugi, M., Kishida, H.: Frictional resistance at yield between dry sand and mild steel. *Soils Found.* **26**(4), 139–149 (1986)
20. Muir, D.W., Kenichi, M.: Changing grading of soil: effect on critical states. *Acta Geotech.* **3**(1), 3–14 (2007)